Dealing with Ion LET Uncertainties: An Application of Generalized Linear Models

Ray Ladbury, NASA -GSFC code 561.4, Greenbelt, MD 20771.

National Aeronautics and Space Administration

Abstract: We propose Generalized Linear Models for understanding errors in SEE rate due to uncertainties in LET of the ion responsible for the event. Applications are suggested and assessed for suitability of treatment by the model.

Introduction: Statement of Problem

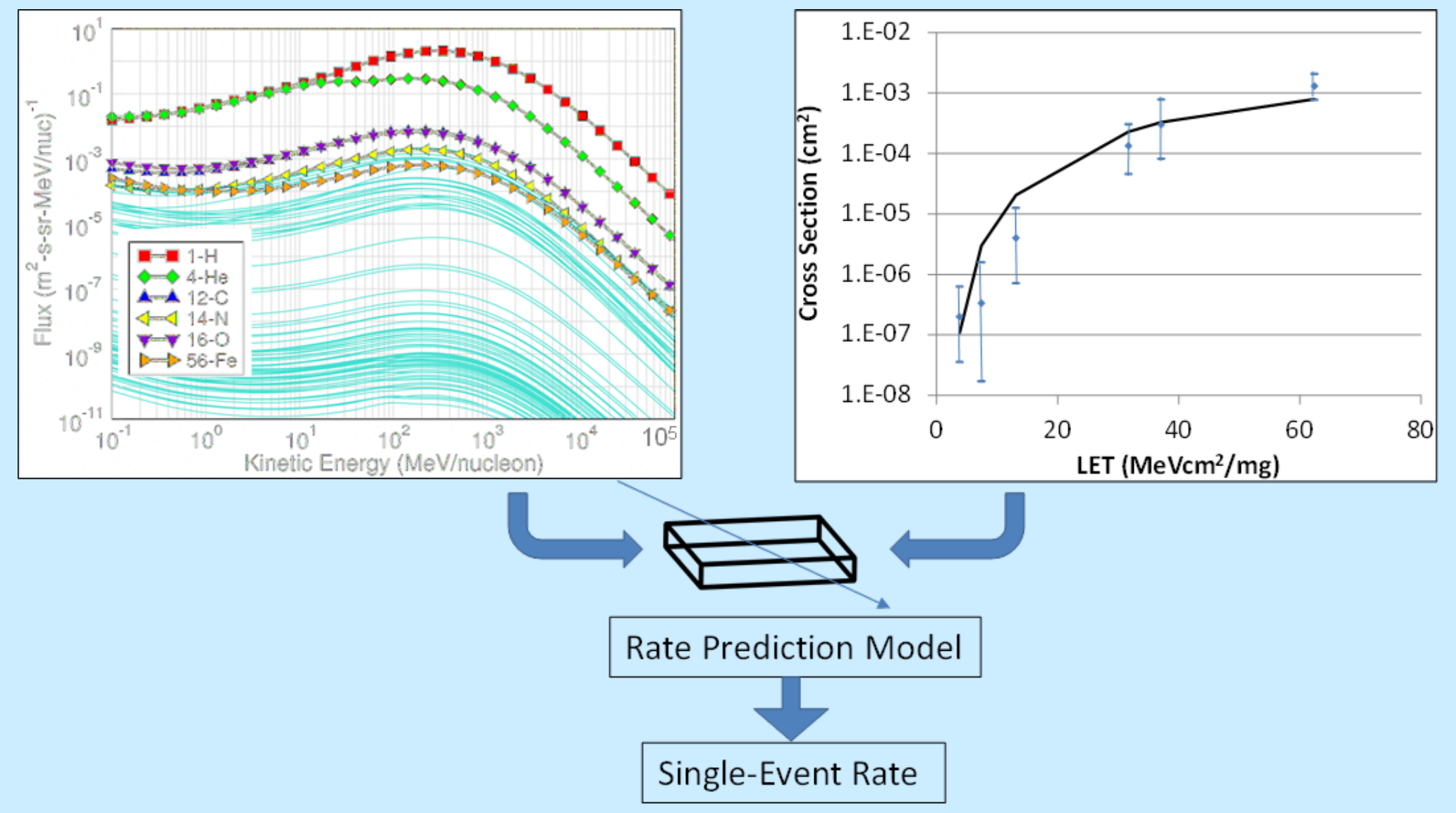

Fig 1. The Rectangular ParallePiped (RPP) approach to Single-Event Effect (SEE) rate estimation fits the SEE cross section σ as a function of Linear Energy Transfer (LET) to a cumulative Weibull (or other) form. The fit is combined with radiation environment models assuming a simplified sensitive volume (SV=RPP) to estimate charge deposited in therein.

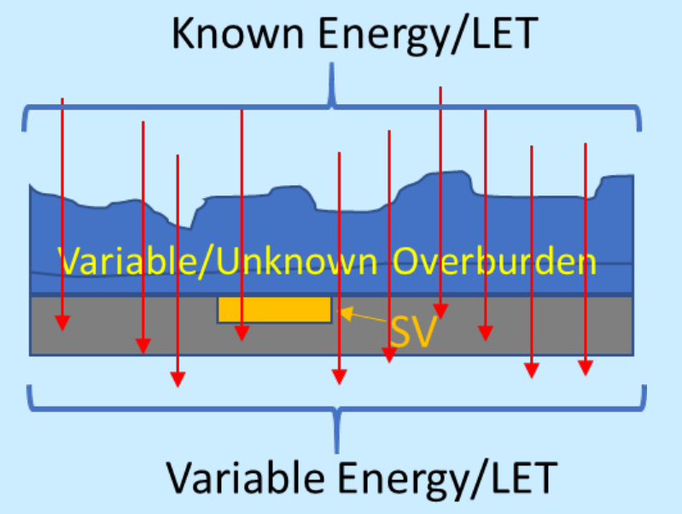

Fig. 2 After traversing nonuniform overburden, uniform energy/LET ion beams will have a range of energies and LET at the SV.

However, in many situations, LET of the ion that causes a given SEE is uncertain, including:

1. Secondary ions from nuclear collisions in the die [1,2] or packaging [3].
2. Space environments [4].
3. Ion beams degraded by traversing nonuniform overburden—e. g. parts thinned for back-side irradiation [5] or packaged parts.
4. Situations where SV dimensions and ion energies render the concept of a single, well-defined LET problematic [6]

LET uncertainties further complicate the difficult task of fitting σ vs. LET data. To date, attempts to deal with LET uncertainties have either limited the role of LET in the analysis[1,2,6] or assigned "representative" LET values for different cross sections [5]. This work instead broadens a Generalized Linear Model (GLM) fitting approach [7] to account for LET uncertainties.

GLMs and SEE Data Fitting

Inputs = Direct Observables:
$\{LET_i\}$, {Fluence=$F(LET_i)$}, {Counts=$N_O(LET_i)$}

Device Response Model for Predicted Counts, N_P
$N_P(LET_i)= F(LET_i) * \sigma_s * Weibull(\Delta LET_i, w, s)$
$\Delta LET_i = LET_i - LET_0$, LET_0 = Onset LET
σ_s = Saturated Cross section
w, s = Weibull width and shape

Statistical Model:
Poisson($N_O(LET_i)$), Mean = $N_P(LET_i)$)
Solve for LET_0, σ_{sat}, w, s that maximize Likelihood, Λ

$$\Lambda = \prod_{i=1}^{n} \text{Poisson}(N_O(LET_i)\}, NP(\Delta LET_i)) \quad (1)$$

Also allows rate to be bounded for a fiven Confidence, CL
Determine confidence contours in LET_0, σ_{sat}, w, s using

$$\frac{\Lambda(CL)}{\Lambda_{Max}} = \exp(-0.5 * INV\chi^2(1 - CL, DOF)) \quad (2)$$

(DOF=# parameters=4. Parameter set inside CL yielding Worst-Case (WC) rate is the bounding rate @ CL.

If LET for i^{th} run is uncertain, ranging $L_i^l \le LET_i \le L_i^u$, the following changes needed to GLM:
1) Must know distribution of ion fluence vs. LET, Φ_i(LET)
2) $N_O(i)$ is now equal to event count observed in i^{th} run and produced by Φi(LET)
3) $N_p(i) = \int_{Ll}^{Lu} \Phi_i(LET) * \sigma_s * Weibull(\Delta LET_i, w, s) dLET$
4) Continue w/ Poisson Likelihood as before.

GLM extend likelihood methods beyond linear probabilistic models. The complex model enters the GLM in terms of the parameters of a probabilistic models from the exponential family—e.g. normal, Poisson exponential, etc.

Likelihood allows one to find not just the best-fit solution, but also bounding fits for any confidence level (CL). Selecting the fit within a given CL contour that yields the highest SEE rate gives the bounding SEE rate consistent with that confidence, e.g. $R_{CL=90\%}$ bounds the rate with at least 90% confidence. The ratio of $R_{CL=90\%}$ to the maximum likelihood (ML) rate (R_{ML}) is a good metric for data quality.

To adapt the GLM to uncertain LET, we modify the equation for N_p by adding an integral over ion fluence vs. LET. The expression for $N_p(i)$ in the lilac square is equivalent to multiplying the total ion fluence by the cross section averaged over the LET distribution. Since $\Phi i(LET_i)$ can be written as the product of the total flux for ion i, Ni, and the probability distribution that the ion has a given LET value, the integral in 3) n in the lilac section is just the product of Ni and average cross section over the LET uncertainty range.

Example: Backside Irradiation of an SDRAM

One common situation where ion LET uncertainty becomes significant arises due to the difficulty of achieving uniform overburden thickness when thinning a die for backside irradiation. We take as an example the use of a GLM to deal with LET uncertainty arising from backside irradiation of a DDR2 SDRAM [7]. Starting with figure 2 from [7], we estimated the proportion of the die falling into each 10-micron thickness bin. Then, using a lookup table constructed using output from SRIM [8], transported representative ion beams from the 15 and 25 MeV/u tunes from the Texas A&M University Cyclotron Facility (TAMU) through these thicknesses to extract the LET distributions in Table I:

TABLE I: LET DISTRIBUTIONS FOR SELECTED TAMU IONS FOR DDR2 EXAMPLE

Thickness, µm	0	30-40	40-50	50-60	60-70	70-80	80-90	95-100
Proportion of die	0	0.11	0.33	0.19	0.18	0.1	0.08	0.02
LET After Overburden (MeVcm²/mg), TAMU 25 MeV Tune								
N@0° to Normal	0.86	0.88	0.88	0.88	0.89	0.89	0.90	0.90
N@45° to Normal	1.22	1.25	1.25	1.26	1.27	1.28	1.29	1.30
N@60° to Normal	1.72	1.78	1.80	1.82	1.84	1.86	1.88	1.90
Ne@0° to Normal	1.73	1.77	1.79	1.80	1.81	1.82	1.84	1.85
Ne@45° to Normal	2.45	2.53	2.55	2.58	2.61	2.64	2.68	2.71
Ne@60° to Normal	3.47	3.63	3.69	3.75	3.81	3.88	3.94	4.01
Ar@0° to Normal	5.60	5.78	5.85	5.92	5.98	6.05	6.12	6.19
Ar@45° to Normal	7.92	8.31	8.45	8.59	8.72	8.86	9.04	9.22
@Ar60° to Normal	11.19	12.04	12.31	12.60	12.96	13.32	13.69	14.13
Xe@0° to Normal	41.77	44.61	45.52	46.52	47.52	48.69	49.85	51.15
Xe@45° to Normal	59.07	65.02	67.02	69.31	71.75	74.48	77.57	81.02
Xe@60° to Normal	83.53	96.20	100.96	106.51	113.04	120.72	129.50	137.51
Cu@0° to Normal	13.35	14.02	14.22	14.45	14.69	14.92	15.19	15.47
Kr@0° to Normal	20.03	21.22	21.61	22.04	22.48	22.95	23.46	23.99
Ag@0° to Normal	32.65	34.93	35.63	36.45	37.30	38.19	39.18	40.26
LET After Overburden (MeVcm²/mg), TAMU 15 MeV Tune								
N@0° to Normal	1.32	1.38	1.40	1.42	1.44	1.46	1.49	1.51
N@45° to Normal	1.87	1.99	2.03	2.08	2.13	2.18	2.23	2.29
N@60°to Normal	2.64	2.91	3.00	3.10	3.21	3.35	3.49	3.66
Ne@0° to Normal	2.59	2.75	2.81	2.86	2.92	2.99	3.06	3.13
Ne@45° to Normal	3.66	4.01	4.12	4.25	4.39	4.55	4.73	4.92
Ne@60°to Normal	5.18	5.91	6.18	6.50	6.86	7.31	7.84	8.52
Ar@0° to Normal	7.90	8.53	8.76	8.99	9.26	9.54	9.84	10.18
Ar@45° to Normal	11.17	12.54	13.03	13.60	14.24	15.00	15.90	16.99
Ar@60°to Normal	15.79	18.80	20.01	21.54	23.53	26.17	30.02	35.86
Cu@0° to Normal	17.98	19.98	20.70	21.53	22.50	23.60	24.91	26.45
Kr@0° to Normal	26.66	29.69	30.71	31.82	33.07	34.39	35.83	37.34
Ag@0°to Normal	42.34	47.89	49.90	52.12	54.49	56.92	58.89	59.04
Xe@0°to Normal	53.14	59.20	61.27	63.47	65.72	67.82	69.21	68.67
Ho@0°to Normal	69.90	75.52	77.29	79.06	80.71	81.93	82.15	80.05
Au@0°to Normal	80.89	86.50	88.31	90.17	91.98	93.54	94.33	93.31

Table I indicates that heavier the ion and the greater the angle of incidence to the normal, the greater the LET uncertainty introduced by nonuniform overburden. However, the behavior of ion flux vs. LET and the rapidity of the rise in cross section vs. LET over the range of LET uncertainty also affect the systematic error magnitude. Moreover, if the data leave important features of device response uncertain (e.g. σ_{sat}, LET_0, etc.), the resulting uncertainty in these parameters can augment the systematic errors due to LET uncertainty. To explore these effects, we carried out Monte Carlo studies of the effect of LET uncertainty coupled with that of Poisson errors on the event counts over a range of Weibull fit parameters.

TABLE II: IONS USED VS. WEIBULL WIDTH, ENERGY

Ions Used Un MC Runs, 25 MeV Tune							
Ion#	1	2	3	4	5	6	7
w=5	N	Ne	Ne@45°	Ar	Ar=@45°	Cu	Xe
w=20	N	Ne	Ar	Cu	Kr	Ag	Xe
w=80	N	Ne	Ar	Kr	Xe	Xe=@45°	Xe=@60°
Ions Used Un MC Runs, 15 MeV Tune							
w=5	N	N@45°	Ne	Ne@60°	Ar	Ar@60°	Xe
w=20	N	Ne	Ar	Cu	Kr	Ag	Xe
w=80	N	Ne	Ar	Kr	Xe	Ho	Au

We chose the 8 ions for each of the runs such that the main features (e.g. σ_{sat}, LET_0 and the rising portion of the curve) of the Weibull form of the cross section were resolved. This meant that rapidly rising cross sections used mainly lower-LET ions and broad curves used more higher LET ions.

Results and Discussion

We began by exploring how Weibull width and ion energy affect systematic errors. We fixed σ_{sat}=.0005 cm², LET_0,=1 MeVcm²/mg and shape s=2. We then varied the Weibull width from narrow (w=5) to medium (w=20) and very slowly saturating (w=80) forms, generating 1000 Monte Carlo events for each run. These runs show that while SEE rates converge even for moderately low event counts, if LET uncertainty is treated improperly, they will converge to the wrong value.

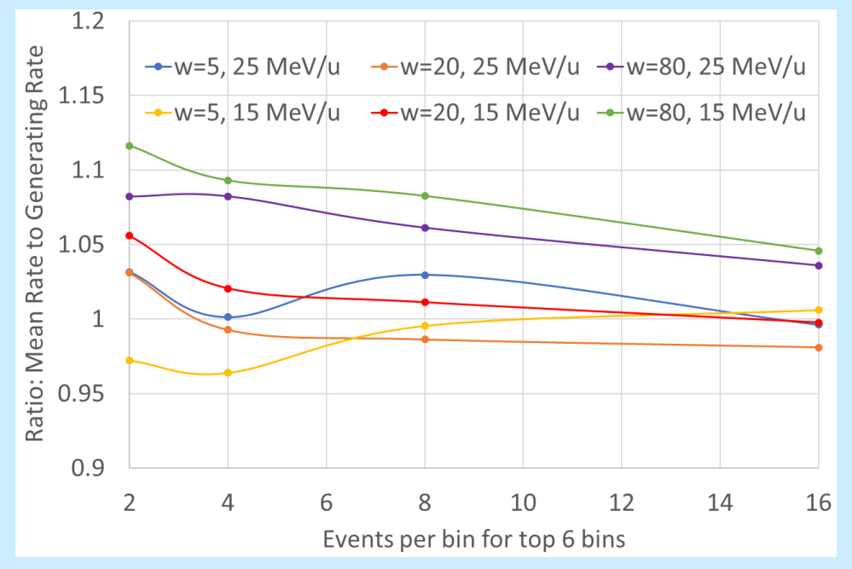

Fig. 3 Even for low event counts (2-16 per cross section), the rate determined by the GLM fit converges on average to the value generated by the Monte Carlo as long as the uncertainty in LET is treated as outlined in section I. Usually, once event counts reach 16 or more, the statistical errors on the predicted rate are only a few percent.

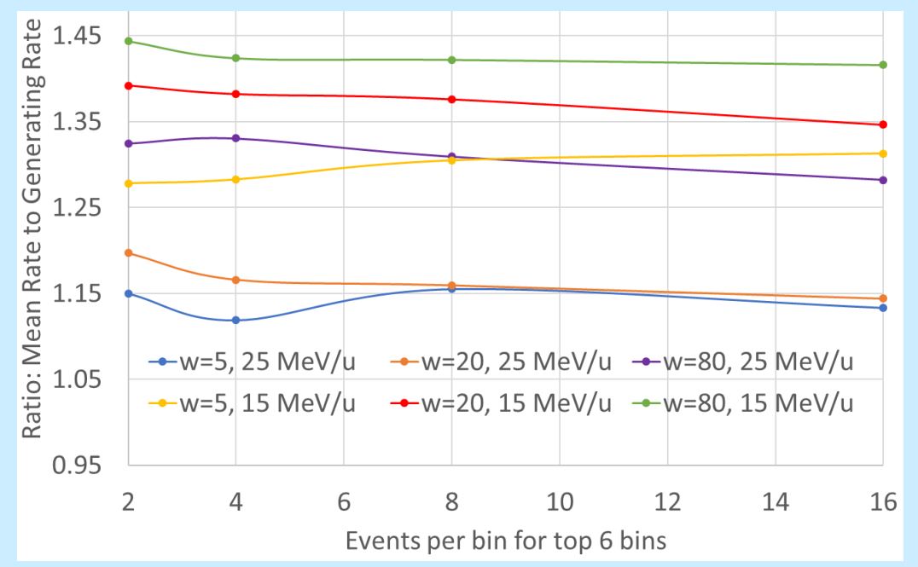

Fig. 4 When LET is uncertain, assigning a single LET value for each cross section introduces a systematic error, so the rate will not converge to the correct value regardless of event count. Because ion energies here remain on the high side of the Bragg peak, ions transiting overburden increases their LET, resulting in overestimated rates.

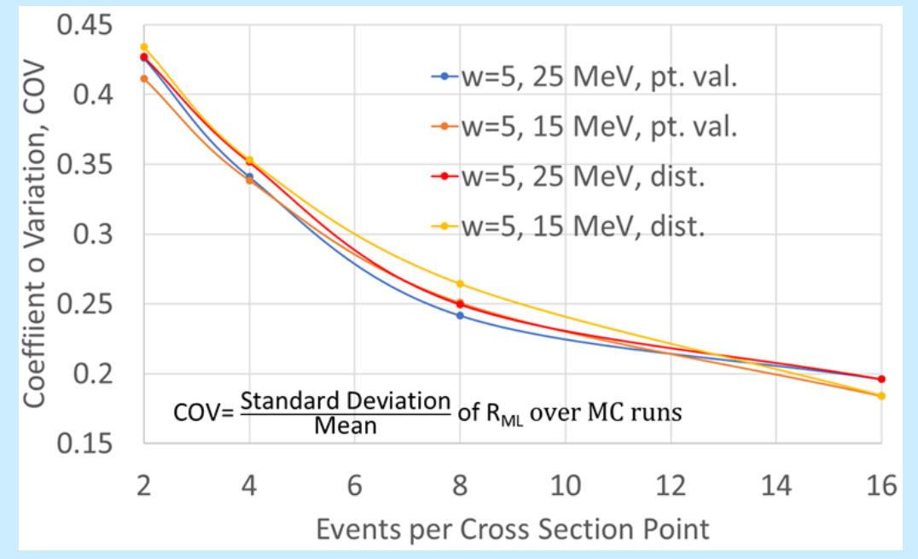

Fig. 5 Systematic errors due to LET uncertainty are largely independent of random (Poisson) errors on event counts, as shown by this plot of COV versus event count. Similar behavior is seen for other generating fit parameters

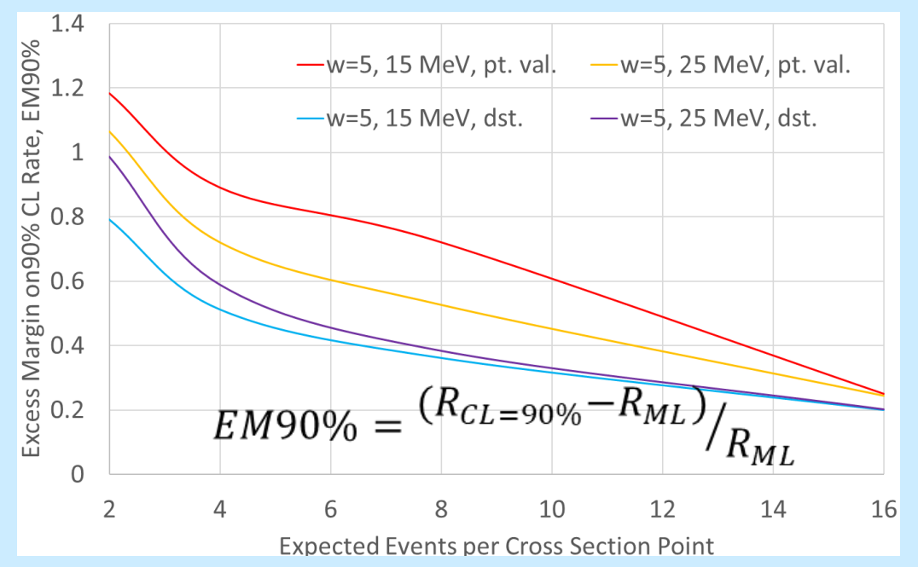

Fig. 6 $R_{CL=90\%}$ serves as a conservative bound on SEE rates. Usually, $R_{CL=90\%}$ bounds the real rate more than 90% of the time. Excess margin (defined in the graph) decreases with event count, but it remains greater than zero.

The main concern when dealing with systematic errors is how large they can get. Fig. 7 illustrates that the magnitude of the errors discussed here is highest when an ion has a large LET uncertainty that overlaps with a region where σ vs. LET is rising rapidly and where the ion flux in the intended environment is not negligible.

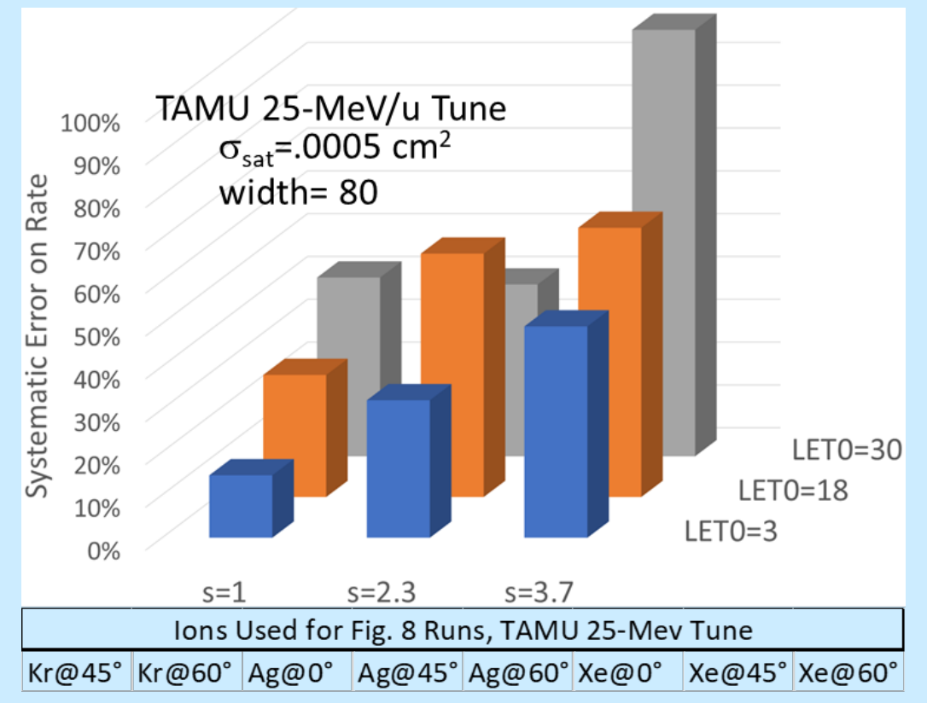

Fig. 7 Broad Weibull forms (w=80) and higher LET0 increase the importance of high-LET ions, where LET uncertainty is higher. Larger Weibull shape s causes σ to rise rapidly at median LET values. In essence, the highest systematic errors (sometimes exceeding the magnitude of the rate) occur when rapid rise overlaps large uncertainty.

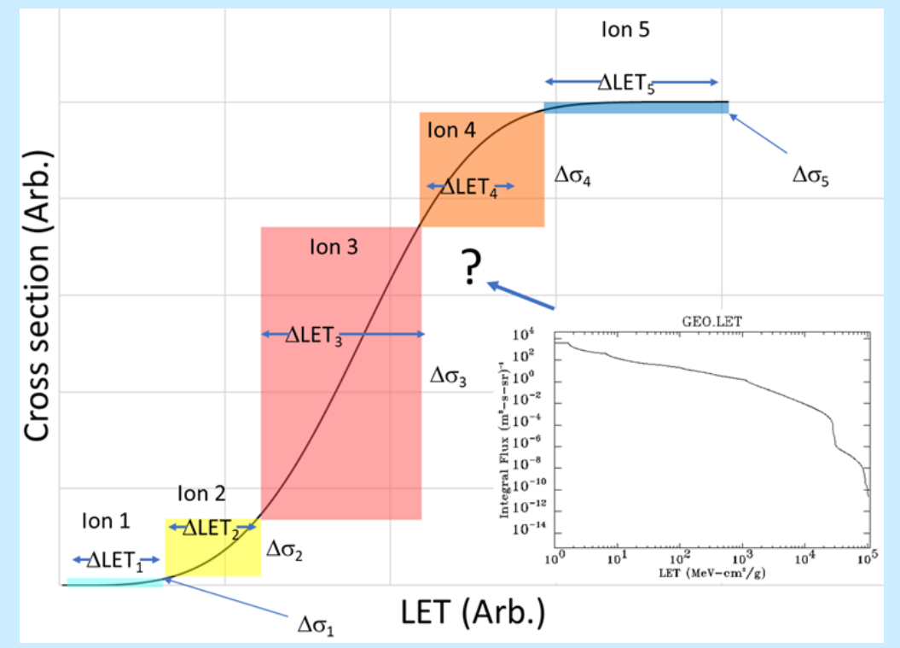

Fig. 8 Systematic errors due to improper LET uncertainty treatment depend on the magnitude of the uncertainty, but also on how rapidly the cross section is rising and how rapidly the environmental ion flux is falling over that uncertainty. The influence of ions 1 and 2 is limited by the small change in cross section, of ion 4 due to the falling ion flux and ion 5 by both.

Although this analysis looked at only one example of LET uncertainty, the results suggest general principles useful for minimizing systematic errors due to LET uncertainties even when precise LET distributions cannot be determined:

1) If ion paths to device sensitive volumes traverse variable overburden, it is important to ensure they remain on the high-energy side of the Bragg peak so that systematic errors do not result in underestimation of error rates.
2) Although higher-energy ions usually have lower LET uncertainty, if one must irradiate at angle to achieve sufficient effective LET to reveal σ_{sat}, the longer ion path lengths can result in higher LET uncertainty for the high-energy beam.
3) If critical features of the σ vs. LET curve—e.g. onset, saturation and steep rise with LET are not well defined in the data, the resulting uncertainty in fit parameters can augment the systematic errors due to LET uncertainty.

Other Applications

Although we have discussed LET uncertainty in the context of backside irradiation of thinned microcircuits, it arises in many other situations. One important example occurs when irradiating packaged microcircuits with an ion beam sufficiently energetic to reach the sensitive volume.

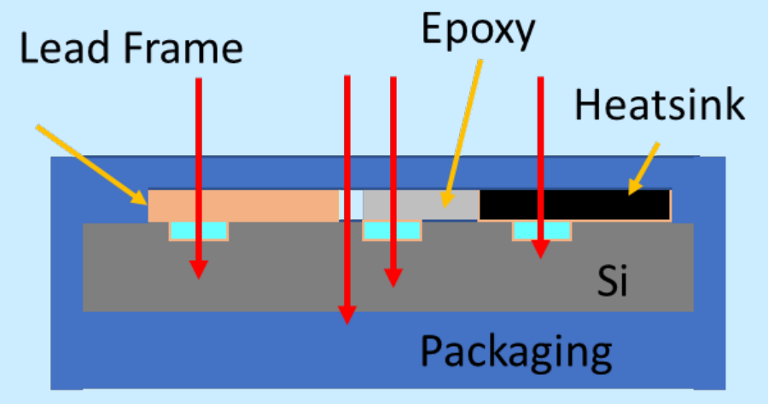

Fig.9 In irradiating packaged parts with high-energy ion beams, different features in the package can result in ions with variable energy/LET reaching the SV.

Sensitive volumes inside increasingly complicated packages may covered by heat sinks, metal lead frames, various epoxies or other fillers and even other die in Systems In Packages. True 3-dimensional monolithic silicon parts, such as 3D NAND Flash memory, are also becoming more complex and possibly less homogeneous.

Additional applications can be found by taking advantage of the concept of volume equivalent LET, LET_{EQ} [12,13]. An ion's LET_{EQ} is defined in terms of the deposited energy E_{dep} in the SV, the SV depth d and the material density ρ

$$LET_{EQ} = {E_{dep}}/{(\rho * d)}$$

In many cases, secondary particles (recoil ions, delta rays) may result in significantly higher and variable E_{dep} for a small proportion of the ions (see Fig. 10).

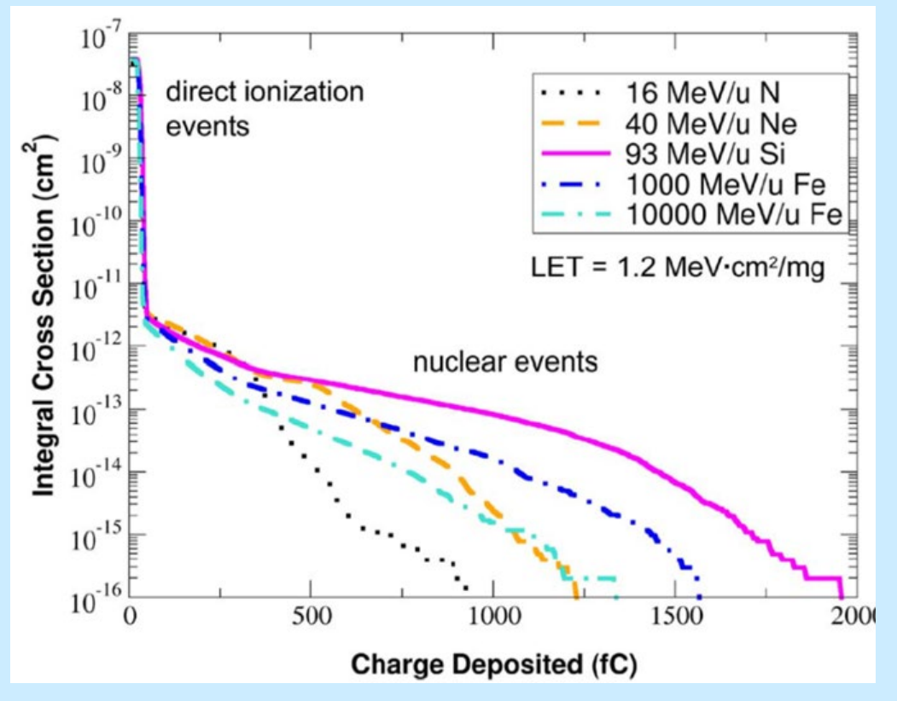

Fig.10 This plot of charge deposited in a representative 2×2×2.25 µm SV for an SRAM from [14] shows that while most events deposit charge/energy consistent with the particles' low LET, some ions generate secondaries in high-Z elements in the die or packaging, resulting in nonzero probability of much higher LET_{EQ}.

Secondary particles can have a significant effect on the cross section especially when the primary ion LET is at or below threshold. A conventional fit to σ vs. LET would be forced incorrectly to choose very low onset LET, whereas use of a LET_{EQ} distribution allows the σ averaged across the distribution to be nonzero even for ion LET below threshold. A similar situation occurs with generation of rare delta rays [15] significantly augmenting the energy deposited in some small SV, especially for very high-energy ions. While such events render use of LET questionable for high-energy ion energy deposition in deep submicron parts, the situation may prove amenable to fitting with use of LET_{EQ} distribution.

Unfortunately, having the capacity to fit σ vs. LET_{EQ} for situations where secondaries are important does not mean that one will have sufficient information to do so. For instance, although high-energy protons generate SEE via p + Si recoil ions with Z from 2-15, and LET up to ~15 MeVcm2/mg, for protons energies (E_p) between 20 and 500 MeV, over 90% of the ions produced have LET_{EQ} well under ~5.5 MeVcm²/mg (for a 1 µm cube), and the total cross section for ions with LET_{EQ} >0.5 MeVcm²/mg varies by only a factor of 2 over this proton energy range). Also, for common proton energies (50<E_p<500 MeV) the proton recoil LET_{EQ} spectrum varies so little that it is not possible to build a piecewise picture of how σ varies with LET as in Fig. 8. Testing with variable proton energy mainly produces recoil ions over the same narrow range of LET_{EQ} (see Fig. 11). Although it is possible that the greater sensitivity of high-Z nuclear reactions could better cover the needed LET spectrum the reaction products are still low-energy, and daughter products of most materials show little dependence on primary energy.

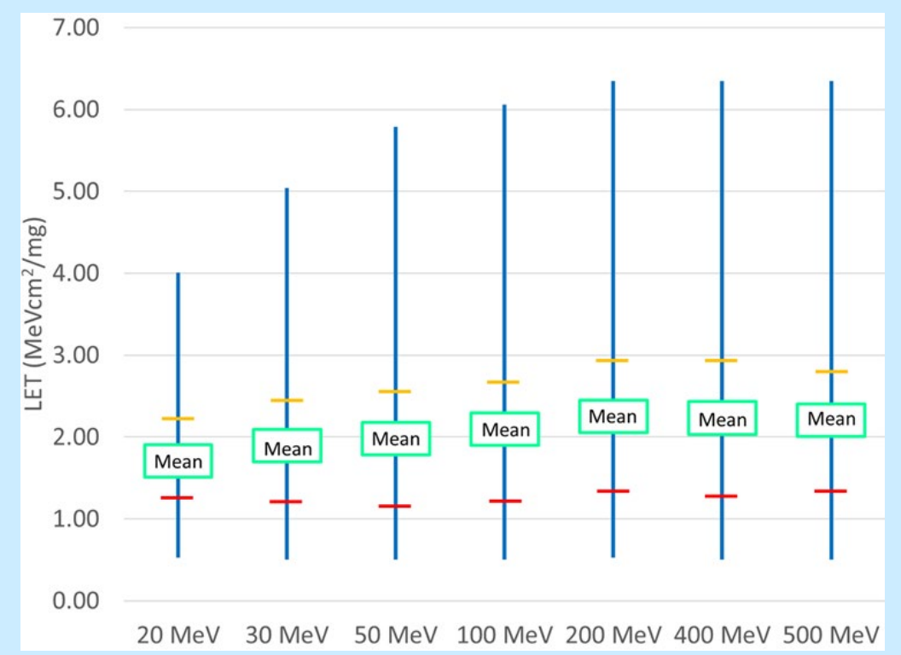

Fig.11 Proton-recoil LET_{EQ} spectrum varies little for usual test energies (20 MeV≤Ep ≤50 MeV). Vertical blue bars encompass 90% of the flux, and red and gold horizontal bars the 50% (median) and 75% quantiles.

Many other situations occur where the ion LET responsible for an SEE is uncertain. These include daughter products of nuclear reactions [3], which could prove amenable to treatment using LET_{EQ}, and even anomalies in the space environment itself, where event rates in various environments (e. g. solar particle events, the South Atlantic Anomaly, etc) can yield insight into device responsible. Indeed, if a program is using large numbers of devices with different sensitivities, changes in the relative rates for such devices could provide insight into the particle content of these different environments.

Conclusions

We have modified the SEE σ vs. LET fitting procedure from [7] to deal with situations where LET is uncertain by replacing point estimates of σ with averages of over the expected LET distribution. A detailed example discusses backside irradiation of a thinned DDR SDRAM, with variable overburden over various device SV. In this example, while use of σ point estimates does not prevent the fit converging as event count increases, it introduces a systematic error with magnitude depending not just on the range of LET uncertainty, but also on the behavior of σ vs. LET over that range. By revealing general dependence of the resulting systematic error, the analysis also yields general principles useful for minimizing systematic error even if the precise LET distribution is not known. The procedure is likely to also be useful when inhomogeneous materials in 3-dimensional packaged microcircuits result in uncertain LET under irradiation with high-energy, penetrating heavy ions.

However, uncertain LET occurs in a variety of other applications, including those where secondary particles contribute significantly to energy deposition in some events, such as proton-recoil ions, nuclear reactions and the production of delta rays especially by very high-energy ions. These problems could also be treated with the approach discussed here using the volume equivalent LET, rather than ion LET.

Acknowledgment

This work was supported in part by the NASA Engineering and Safety Center (NESC).

References

[1] D. M. Hiemstra and E. W. Blackmore, "LET spectra of proton energy levels from 50 to 500 MeV and their effectiveness for single event effects characterization of microelectronics," IEEE Trans. Nucl. Sci., vol. 50, no. 6, pp. 2245–2250, Dec. 2003.

[2] P. O'Neill, G. Badhwar, and W. Culpepper, "Risk assessment for heavy ions of parts tested with protons," IEEE Trans. Nucl. Sci., vol. 44, pp. 2311–2314, Dec. 1997.

[3] T. L. Turflinger et al.., "RHA implications of proton on gold-plated package structures in SEE evaluations," IEEE Trans. Nucl. Sci., vol. 62, no. 6, pp. 2468–2475, Dec. 2015.

[4] R. Ecoffet (2007) "In-flight Anomalies on Electronic Devices,". In: R. VELAZCO, P. FOUILLAT and R. REIS (eds.) Radiation Effects on Embedded Systems. Springer, Dordrecht. https://doi.org/10.1007/978-1-4020-5646-8_3

[5] R. Harboe-Sørensen, E, F.-X. Guerre, and G. Lewis, "Heavy-Ion SEE Test Concept and Results for DDR-II Memories," IEEE Trans. Nucl. Sci. vol. 54, no. 6, pp. 2125-2130, Dec. 2007.

[6] S. L. Weeden-Wright et al., "Effects of Energy-Deposition Variability on Soft Error Rate Prediction," IEEE Trans. Nucl. Sci. vol. 62, no. 5, pp. 2181-2186, Oct. 2015.

[7] R. Ladbury, "Statistical properties of SEE rate calculation in the limit of large and small event counts," IEEE Trans. Nucl. Sci., vol. 54, no.6, pp. 2113–2119, Dec. 2007.

[8] J. F. Ziegler, et al. The Stopping and Range of Ions in Matter. Available: http://www.srim.org, (1/23/2021)

[9] William G. Wong, "3D NAND Hits 176 Layers," Dec. 15, 2020 https://www.electronicdesign.com/technologies/embedded-revolution/article/21148162/electronic-design-3d-nand-hits-176-layers

[10] M. Bagatin et al., "Effects of Heavy-Ion Irradiation on Vertical 3-D NAND Flash Memories," IEEE Trans. Nucl. Sci., vol. 65, no.1, pp. 318–325, Jan. 2018.

[11] C. C. Foster et al., "Certification of Parts for Space With the Variable Depth Bragg Peak Method," IEEE Trans. Nucl. Sci., vol. 59, no.6, pp. 2909–2913, Dec.. 2012.

[12] R. Ladbury, J.-M. Lauenstein and K. P. Hayes, Use of Proton SEE Data as a Proxy for Bounding Heavy-Ion SEE Susceptibility, IEEE Trans. Nucl. Sci., Vol. 62, No. 6, p. 2505 – 2510, Dec. 2015

[13] R. Garcia-Alia et al., "Simplified SEE sensitivity screening for COTS components in space," IEEE Trans. Nucl. Sci., vol. 64, no. 1, pp. 301–308, Feb. 2017.

[14] N. A. Dodds et al., "Charge generation by secondary particles from nuclear reactions in BEOL materials," IEEE Trans. Nucl. Sci., vol. 56, no. 6, pp.3172–3179, Dec. 2009.

[15] M. P. King et al.,"The impact of delta-rays on single-event upsets in highly scaled SOI SRAMs,"IEEE Trans. Nucl. Sci., vol. 57, no. 6, pp. 3169–3175, Dec.2010.

To be presented virtually by Raymond L. Ladbury at the Institute of Electrical and Electronics Engineers (IEEE) Nuclear and Space Radiation Effects Conference (NSREC), virtual, July 16-23, 2021 and published on nepp.nasa.gov.